IEEE Photonics Journal
An IEEE Photonics Society Publication

Open Access

GaN-Based Generic Bifunction LED for Potential Duplex Free-Space VLCs

Volume 9, Number 5, October 2017

Lilin Liu
Xiangying Zhang
Zhenkun Sun
Bing Yan
Dongdong Teng
Gang Wang

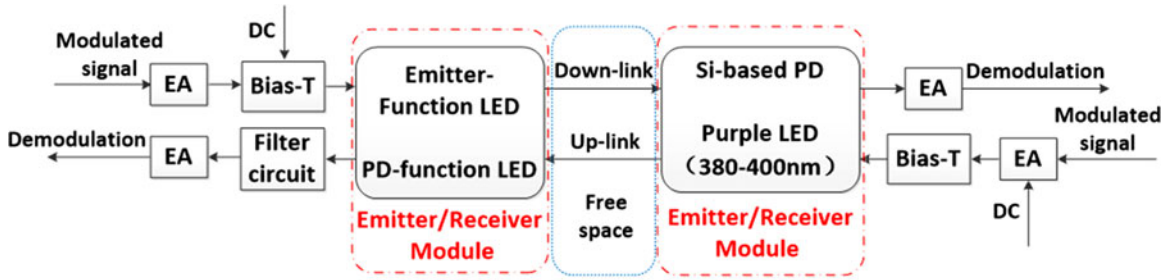

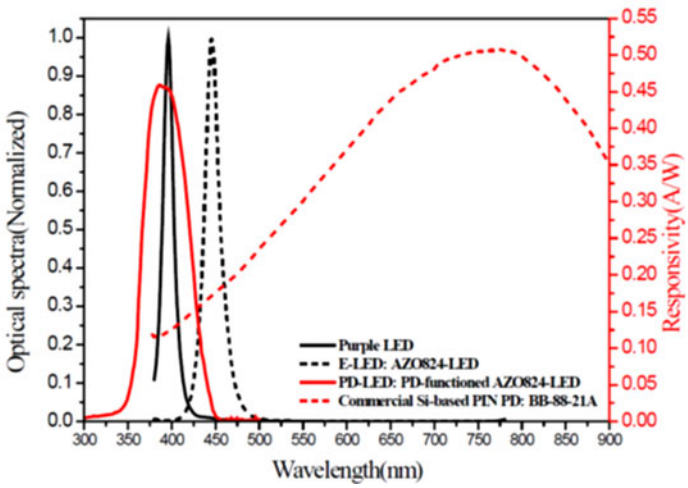

DOI: 10.1109/JPHOT.2017.2733039
1943-0655 © 2017 IEEE

IEEE photonics SOCIETY

IEEE

GaN-Based Generic Bifunction LED for Potential Duplex Free-Space VLCs

Lilin Liu,[1] Xiangying Zhang,[1] Zhenkun Sun,[1] Bing Yan,[1] Dongdong Teng,[2] and Gang Wang[1]

[1]School of Electronics and Information Technology, Sun Yat-Sen University, Guangzhou 510275, China
[2]School of Physics, Sun Yat-Sen University, Guangzhou 510275, China

DOI:10.1109/JPHOT.2017.2733039

Manuscript received April 12, 2017; revised July 3, 2017; accepted July 5, 2017. Date of publication July 28, 2017; date of current version August 14, 2017. This work was supported in part by the Guangdong Technical Plan under Grants 2016B010111002, 2014B010119003, 2014B010122005, and 2015B010113002, in part by the "863" Program of China under Grant 2015AA03A101, in part by the Guangzhou Technical Plan Project under Grant 201510010280, and in part by the opening project of Guangdong Provincial Key Laboratory of Electronic Information Products Reliability Technology under Grant 2013A061401003. Corresponding authors: L. Liu and D. Teng (e-mail: liullin@mail.sysu.edu.cn; tengdd@mail.sysu.edu.cn).

Abstract: A generic bifunction GaN light-emitting diode (LED) structure, which has a 300 nm n^+-*ZnO* epitaxial layer grown on a standard GaN LED epistack and a mesa size of 200 μm $\times$ 600 μm, exhibits a peak responsivity of 450 mA/W to purple lights (380–400 nm) under zero bias and a narrow bandpass of around 60 nm. The corresponding product of quantum efficiency and gain is estimated as 140%. The purple light (380–400 nm) to blue light ($>$460 nm) rejection ratio can reach two orders of magnitude. The generic bifunction LED does not sacrifice its optical and modulation performances as a light transmitter. The optical power reaches 100 mW with a peak wavelength around 447 nm. A new proposition for duplex free-space visible light communications is depicted.

Index Terms: Light-emitting diode (LED), free space visible light communication (VLC), visible light photodetector.

1. Introduction

InGaN-based blue light-emitting diodes (LEDs) achieve growing interests due to the great potential to realize energy efficient general lighting and high speed free-space visible light communication (VLC) simultaneously [1]–[6]. The VLC offers many advantages over radio-frequency (RF) communication [1]–[6], such as license-free bandwidth, simple front-end devices, no interference with sensitive electronic equipment, the usage of existing lighting infrastructure, *et al.*.

In the record-breaking era, lots of researches were committed to increase data rates of VLC systems. Most researches were conducted on downlink signal transmission. Advanced algorithms were developed to enhance data rates. White light sources based on RGB LEDs emerged as an approach for general lighting [7], [8]. Combining high order quadrature amplitude modulation (QAM) and wavelength division multiplexing(WDM), data speeds of 2.5 Gb/s with orthogonal frequency division multiplexing (OFDM) [9], 3.4 Gb/s with discrete multitone (MDT) [5], 4.22 Gb/s with single carrier frequency domain equalization (SC-FDE) [10], and 4.5 Gb/s with carrier-less amplitude and phase modulation(CAP) [11] were reported. More recently, employing high order CAP modulation

and hybrid post equalizer, a data rate of 8 Gb/s was reported based on the RGBY LED module [12]. Phosphor-converted white LEDs are more popular in general lighting for cost consideration. C. H. Yeh *et al.* increased the total data rate in phosphor-LED VLC wireless system by dividing the OFDM into multiple bands and supplying them to different LED chips [13]. Through adjusting the number of OFDM subcarriers and using equalization in OFDM, C. W. Chow *et al.* circumvented the background optical noises and enhanced the capacity of the bandwidth-limited LED optical wireless communication link [14]. As an alternative to LED, the coherent blue-laser diode (LD) was combined with a remote phosphor-film for generating white light and boosting the data rate of VLC [15], [16]. Data rates as high as 5.2 Gb/s for one channel were reported over a 60 cm free space link based on 16-QAM OFDM [16]. In addition, many other methods were reported to extend the -3 dB modulation bandwidth of high power white LEDs, such as high performance blue filter, pre-equalization, post-equalization, etc. In 2015, Huang *et al.* proposed a novel cascaded bridged-T amplitude equalizer circuit to extend the -3 dB bandwidth of a commercially available phosphorescent white LED to 366 MHz [17]. A data rate of 1.6 Gb/s was realized by 16 QAM-OFDM at a distance of 1 m. Wang *et al.* developed a high performance blue filter with an average transmittance of 97.5% in the $430-485$ nm and a wide stopband from 500 to 1050 nm [18], which helped breaking the record of VLC system to 2.0 Gb/s at a distance of 1.5 m by using a commercialized 1 W phosphorescent white LED [19].

Duplex communication is a basic requirement of most application scenarios. However, a challenge regarding free space VLC applications is bidirectional communications [20], [21], especially in the case of indoor applications. Most indoor devices do not have a lighting function for data transmission. The usage of a second communication technology, e.g., RF or Infra-red for data uploading was proposed to solve this problem. The drawback lies in the need of a more complex design. Besides, Infra-red laser lights will be harmful to human eyes. VLC usage in vehicle applications is relatively not so problematic, since all the involved equipment can give out lights. Duplex free-space VLC progresses very slowly. The key reason lies in the absence of suitable optoelectronic devices. Existing solutions for duplex free-space VLCs are based on RGB LEDs through wavelength division multiplexing (WDM) [22], [23]. The downlink signals were carried by the red and green emitters, whereas the uplink signals were by the blue emitter. Both the downlink and uplink employ Si-based avalanche or PIN photodiodes (PDs) to receive the modulation signals. Generally, Si-based PDs have wideband frequency response, from near-ultra-violet to near-infra-red. The peak responsivity locate at around 780 nm. In a wide range $470\,\text{nm}-960\,\text{nm}$, the responsivity is larger than 0.2 A/W. At the peak wavelengths of blue($\sim$460 nm) and red($\sim$620 nm) LEDs, the responsivity are 0.15 A/W and 0.4 A/W, respectively. Thus, to increase the robustness to noises, color filters are needed to minimize the crosstalk between downlink and uplink. Such a design strategy for duplex free-space VLC will occupy big spatial volume and be accompanied by high cost and high complexity at both ends.

In order to compete with the radio, low-cost VLC solutions are necessary. Besides, the size of a cell in wireless communication systems has been constantly shrinking over the last decades. Monolithic integration of the light emitter and the photo-detector on a single chip could feature low cost, simplicity, and miniaturization. Integrating GaN-based LEDs and GaN Schottky barrier PDs on a single chip was attempted by Jiang *et al.* [24]. The PD was visible-blind and exhibited a maximum responsivity of 0.2 A/W at 365 nm under -10 V bias. The effective area of the PD was $127\,\mu\text{m} \times 20\,\mu\text{m}$. The 365 nm wavelength is out of the visible light range and maybe harmful to human eyes. An LED itself could be used as a light detector [25]. Quantum-well structures didn't attract exploitation interests in terms of responsivity until Capasso *et al.* [26] identified the mechanism of effective mass filtering, which could lead to large photocurrent gain and, in turn, very high responsivity. Rivera *et al.* [27] experimentally indicated that a huge gain can be achieved using InGaN/GaN multi-quantum-well (MQW) structure embedded in GaN-based p-n junction photodiodes. Pereiro *et al.* [28] obtained a 0.1 A/W responsivity with a detection edge at 450 nm through optimizing the InGaN-GaN MQW structure. G. Stepniak *et al.* [29] recently demonstrated the experimental operation of a wireless transmission link employing identical red LEDs both as transmitter and receiver, which showed a 100 Mb/s speed based on a simple, two-level pulse amplitude

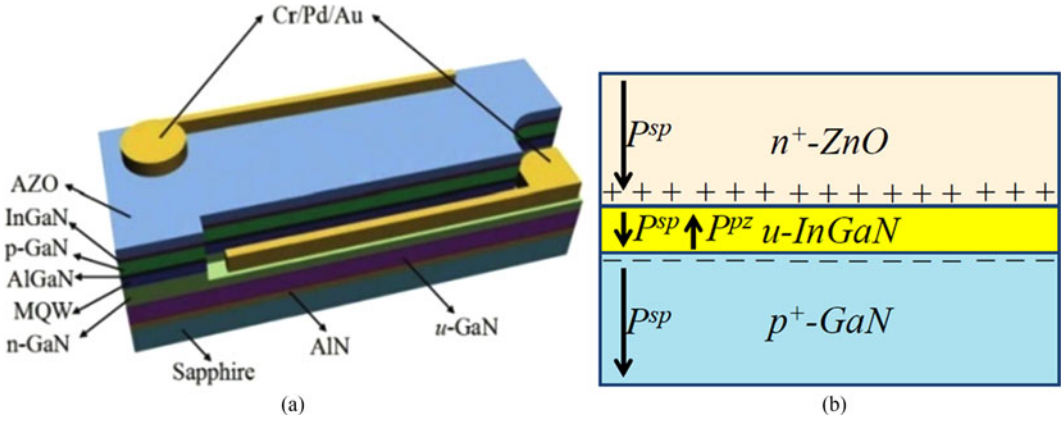

Fig. 1. (a) Schematic drawing of the LED with an AZO-TCL; (b) Polarization states in the p^+-*GaN/u-InGaN/*n^+-*ZnO* sandwich structure.

modulation. Although the induced photo-current in such a commercial LED is very small, limiting the transmission distances and speeds, it is an excited report for VLCs.

The generic structures of LEDs and MQW PDs have similarity. In this letter, a prototype bi-function LED is designed, which has a 300 nm n^+-*ZnO* epitaxial layer grown on a standard GaN LED epi-stack and has a mesa size 200 μm $\times$ 600 μm. As a light receiver, a highest responsivity to 380 $\sim$ 400 nm visible purple lights is obtained for the state of art, to the best of the authors' knowledge. As a light emitter, based on a fix-rate OFDM modulation scheme without pre-equalization, a speed 1.5 Gb/s is demonstrated with a maximum optical power around 100 mW and a peak wavelength around 448 nm. A new proposition for duplex free-space VLCs is depicted and the inadequacies are discussed for future research consideration.

2. Experimental Details

The LED structures are grown on c-plane sapphire substrates by MOCVD. Similar as commercial available LEDs, the epi-structures consist of an AlN nucleation layer, an u-GaN buffer layer, a Si-doped GaN layer, InGaN/GaN MQWs, an AlGaN current blocking layer, a Mg-doped p-type GaN layer and an InGaN contact layer. The unintentional doped InGaN/GaN MQW layer consists of a number of periods of 2.7 nm-thick InGaN well layer and 11.5 nm-thick GaN barrier layer. For the InGaN/GaN MQWs, the "indium" content is designed to be 14.4%. The thicknesses of InGaN and GaN are set to make the InGaN layer be appropriately strained. Mismatch strain induced polarization will shift the light emission peak to around 450 nm. At the same time, a 14.4% of indium is expected to correspond with a light responsivity peak at around 400 nm with a narrow FWHM. So, the emission wavelength and response wavelength can be separated with each other. But the piezoelectric fields can't be too large in order to obtain a relatively sharp absorption edges.

Then, the wafer is transferred to another MOCVD system (MD 600 A 38 $\times$ 2 "MOCVD). A 300 nm-thick aluminum-doped zinc oxide (n^+-*ZnO*) transparent current spreading layer (i.e., AZO-TCL) is grown epitaxially on the top of the contact layer by a developed two-step process. The AZO-TCL plays great roles on improving the modulation capability of light-emitter LEDs [30] and the responsivity of PD-functioned LEDs.

The bi-function LED is designed to have a rectangular mesa: 200 μm $\times$ 600 μm (i.e., 8 mil $\times$ 24 mil, 1 mil $=$ 25 μm), as shown in Fig. 1(a). At present, LEDs with a medium power around 0.2 $\sim$ 0.5 W have become a main stream product. LEDs with other mesa sizes are fabricated as control samples. A wet etching is carried out to pattern the AZO-TCL layer. Reactive-ion etching and inductively coupled plasma etching (RIE-ICP) are used to define the active mesa. Then, Cr/Pd/Au layers are deposited by e-beam evaporation on the n-GaN and mesa as the n-ohmic

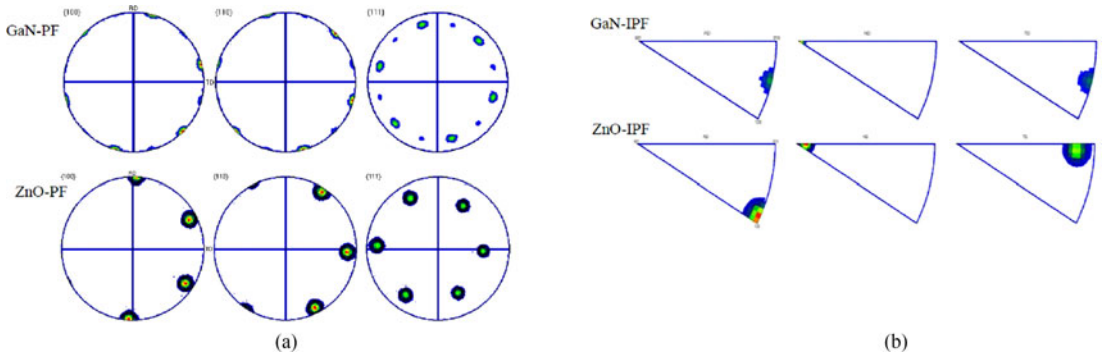

Fig. 2. (a) {100}, {110} and {111} pole figures of p-GaN and n^+-*ZnO*; (b) The RD, ND and TD inverse pole figures of p-GaN and n^+-*ZnO*.

contact and p-ohmic contact, respectively. The designed bi-function LED is denoted as AZO824-LED in the following parts.

Each single LED chip is bonded on a commercial pre-plated leadframe package (5730#) through white glue. The packaged LED devices are soldered on a printed circuit test board by the surface mounting technique. Except for the normal encapsulating silicone lens of the LED, no additional optics is adopted.

3. Epitaxial-Like n+-ZnO Layer Formed on the LED Epistack

The n^+-*ZnO* is confirmed to have an epitaxial-like excellent interface with the LED epi-stack. The crystal structure and orientation are first analyzed by electron backscatter diffraction (EBSD). Using the Zeiss SUPRA55 field emission Scanning Electron Microscopy (SEM) equipped with HKL-Channel.5-EBSD, the {100}, {110} and {111} pole figures and the RD, ND and TD inverse pole figures of the p-GaN and n^+-*ZnO* layers are measured, as shown in Fig. 2(a) and (b). The space resolution is at the scale of 50 nm. The scanning area is set as 200 μm $\times$ 200 μm. The step sizes for p-GaN and n^+-*ZnO* scanning are set as 500 nm and 20 nm, respectively. The magnifications for p-GaN scanning and n^+-*ZnO* scanning are 1000 and 10000, respectively. The orientation rotation is due to the placement of samples in SEM. It can be seen that the points in the pole figures of p-GaN are smaller than those of n^+-*ZnO*, indicating that the crystal quality of n^+-*ZnO* is inferior to that of p-GaN. But, these figures display the same 6-fold symmetry, indicating that the n^+-*ZnO* and p-GaN share the same in-plane crystal orientation.

The cross-section microstructure of p-GaN/InGaN/n^+-*ZnO* interface is analyzed by FEI Tecnai G2 F20. Transmission electron microscopy (TEM) samples were prepared by focused ion beam (FEI Helios) cutting for cross-section investigation, followed by ion milling down to electron transparency. Two locations 1 and 2 are chosen randomly on the bright field TEM image, see Fig. 3(a). Their selected area diffraction (SAD) patterns are shown in Fig. 3(b), confirming very good orientation matching between p-GaN and n^+-*ZnO*. The high-resolution TEM pattern in Fig. 3(c) exhibits good interface states. The X-ray diffraction spectrum in Fig. 3(d) shows that the FWHM of the n^+-*ZnO*(0002) ω-scan is around 2°, indicating nearly epitaxy with quite a few low angle mosaicity in the out-of-plane orientation.

All these results imply that the n^+-*ZnO* film does form epitaxial relationship with the nearly same in-plane and out-of-plane orientation as the p-GaN layer. The excellent interface helps to form a hetero p-n junction and also is expected to decrease the noises related with carrier trapping/de-trapping and scattering at the p electrodes.

The contact resistance can represent the cascade resistance of the p-GaN/InGaN/n^+-*ZnO* structure, which is measured as low as $2.86 \times 10^{-4} \Omega \cdot \text{cm}^2$ through circular transmission line method (CTLM). This value is at the same order with the GaN/GdN/GaN tunnel junction reported by FathihAkyol(2013) [31]. Such a low resistance contributes to the relatively low voltage drop of

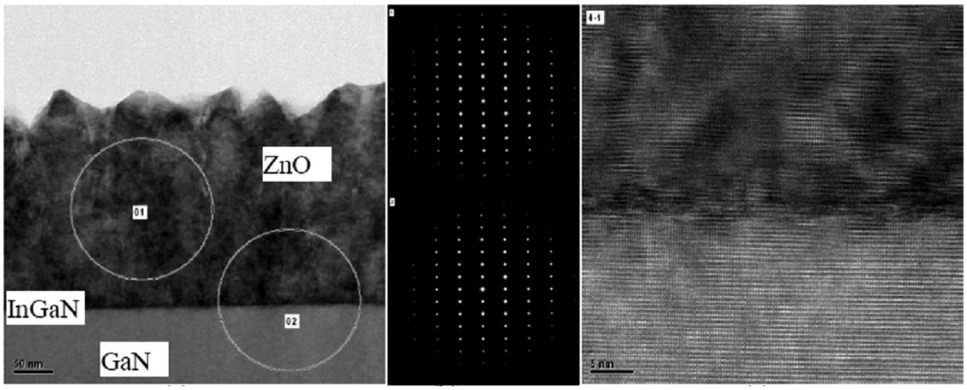

(a) (b) (c)

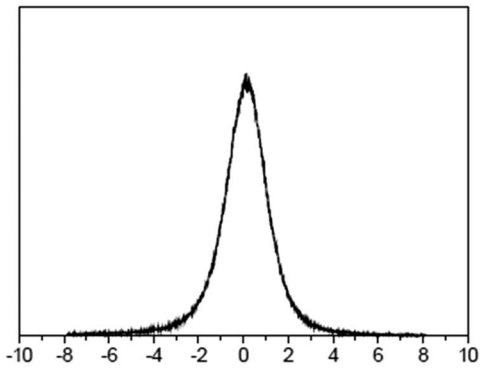

(d)

Fig. 3. Cross-section bright field TEM image (a), SADs of places 01 and 02 (b), and high-resolution TEM image (c) of the *p-GaN/u-InGaN/n*$^+$*-ZnO* structure; (d) the *n*$^+$*-ZnO* (0002) ω-scan.

TABLE 1
The Capacities of LEDs with Different TCLs at the Frequency 1 MHz

Capacity(pF)	AZO824	AZO TCL	Ni/Au TCL
@ −5 V	28.9	72.17	930.56

4.6 mV for a current density 160 mA/mm^2 and a voltage drop of 38 mV for a current density 1.3 A/mm^2. When the LED is forward biased, the hetero p-n junction gets reverse biased, electrons in the valence band of p-GaN layer tunnel into empty states available in the *n*$^+$*-ZnO*, leaving behind a hole in the p-GaN layer. The holes regenerated at the p side of the tunnel junction are injected into the multi-quantum wells of LED, which may promote the radiative recombination process, i.e., B in the ABC model.

The adding of the hetero p-n junction on the standard LED epi-stack can greatly decrease the capacity of LEDs. Table 1 compares the measured capacities of fabricated control sample LEDs with AZO TCL or Ni/Au TCL at −5 V. The scanning frequency is set as 1 MHz. All the control LEDs have the same mesa size, 1 mm × 1 mm. For example, the capacity of a control LED with

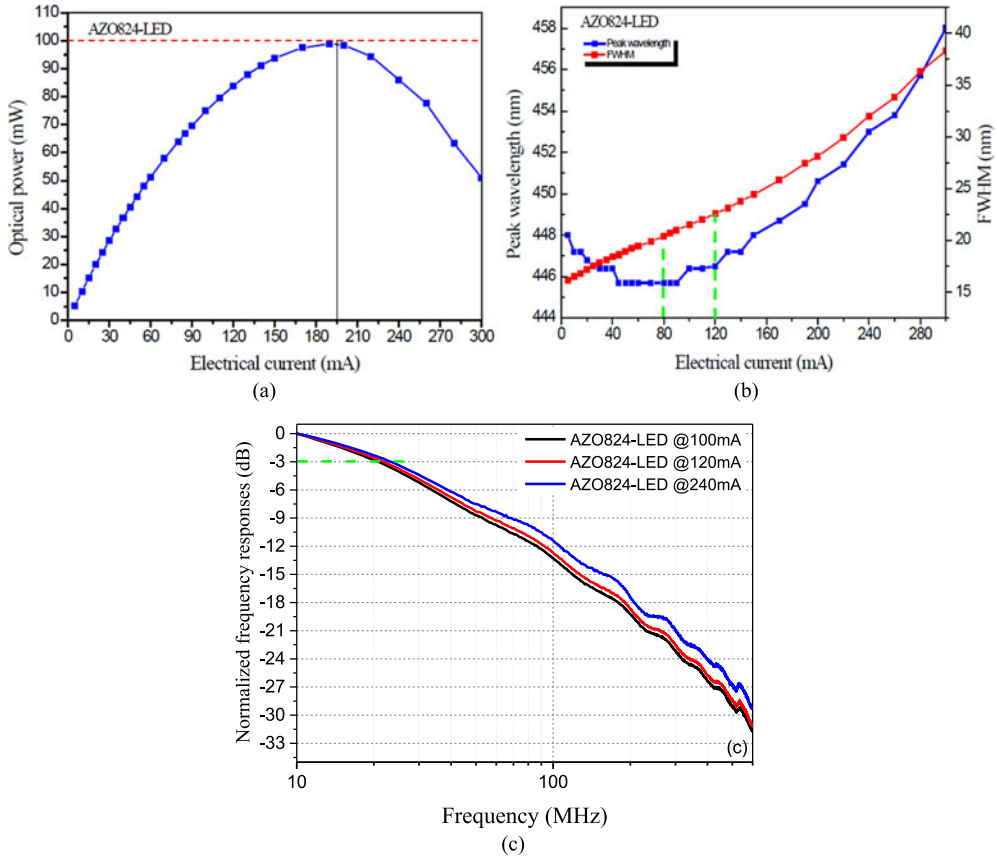

Fig. 4. (a) Curves showing the optical power as a function of the electrical currentsforAZO824-LED; (b) plotting the evolution of peak wavelengths and the full width at the half maximum (FWHM) with the DC electrical currents of the fabricated AZO824-LEDs; (c) Normalized frequency responses of AZO824-LED.

Ni/Au TCL is around 13 times of that with AZO TCL. For the experimental sample AZO824-LED, the capacity is 28.9 pF@ -5 V.

4. Optical Properties of AZO824-LED as a Light Emitter

The turn-on voltage of AZO824-LEDs (I $=$ 10 μA) is measured as 2.46 V. The emission wavelength is about 447 nm under the forward current 20 mA at an ambient temperature of 25 °C. Experimentally, the maximum constant DC current the fabricated AZO824-LEDs can sustain is 195 mA, beyond which the optical power will saturate, as shown in Fig. 4(a). Fig. 4(b) plots the evolution of peak wavelengths and the FWHM with the input DC electrical currents. Within 80$\sim$120 mA, the peak wavelength is around 446 nm and the FWHM is 22 nm. The highest optical power is around 100 mW. The optical power can be increased further.

A transmitter-receiver VLC system is set up to characterize the frequency responses of LEDs by a network analyzer (Agilent N5230 C: 10 MHz–40 GHz). Fig. 4(c) depicts the normalized frequency response of the AZO824-LED. The -3 dB modulation bandwidth is around 10 MHz@100 mA, much smaller than the theoretical value estimated by $f_{-3dB} = 1/2\pi RC$. Further increasing the current level, the 3 dB bandwidth only increases very little. But the 3 dB modulation bandwidth can't represent the real communication capability of LEDs [30].

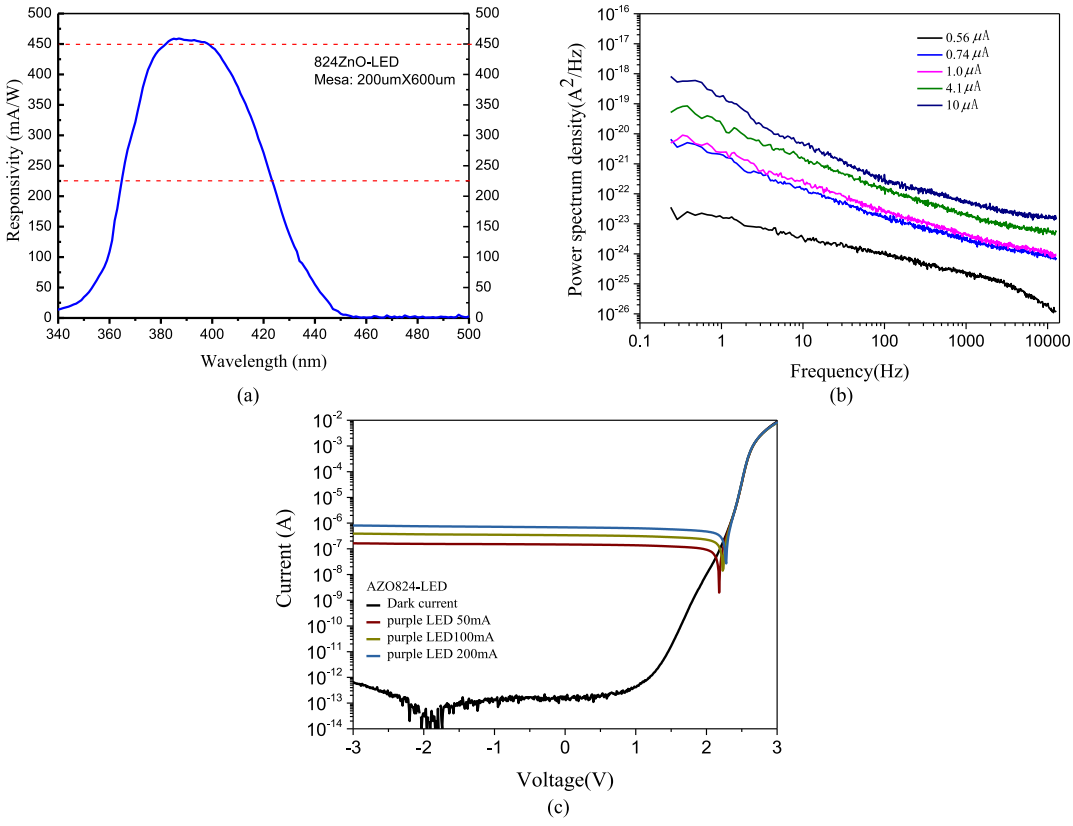

Fig. 5. (a) Spectral response of PD-functioned AZO824-LED at zero bias; (b) The noise power spectrum densities at different input currents; (c) Dark and photocurrents of the AZO824-LED as a function of the voltage under 395 nm illumination. The 395 nm lights are provided by a commercial purple LED at different input currents.

5. Spectral Responsivity of AZO824-LED as a Photodetector

The dark I-V characteristics of the devices are measured with a Keithley 4200 semiconductor characterization system. The optical response characteristics is recorded by a source-measurement unit analyzer (Keithely 2200), using a Xe lamp (150 W) as the light source. The optical power meter (OPHIR) is qualified with a factory calibration, and the spectrometer is calibrated using a standard mercury lamp. The source-measurement unit analyzer (Keithely 2200) is also calibrated before use.

Fig. 5(a) shows the spectral response of the AZO824-LED as a photodetector at zero bias. Within the range of 380 $\sim$ 400 nm, the responsivity values are around 450 mA/W, the corresponding product of quantum efficiency and gain is estimated as 140%. Note that the purple light (380 $\sim$ 400 nm) to blue light ($>$460 nm) rejection ratio can reach two orders of magnitude. To the best of authors' knowledge, the obtained responsivity at 380 $\sim$ 400 nm is highest for the state of art. When a reverse bias is applied, the responsivity presents some extent decrease. Although the photo-response curve doesn't exhibit very steep edges, clear double side cut-off wavelengths can be seen and a narrow band-pass of around 60 nm (i.e., 425 $\sim$ 365 nm) is obtained here. More interesting, the overlap between the electroluminescence (EL) spectrum and responsivity spectra is very limited, which is expected to induce in small crosstalk.

The fabricated AZO824-LED exhibits very small low frequency electrical noises. Fig. 5(b) plots the noise power spectrum densities at different input currents. At each current level, the curves present typical *1/f* low frequency noise characteristics, indicating the fabricated AZO824-LED has good device qualities. Taking the noise power level at 10 Hz for comparison, it can be seen that up to 10 μA, the low frequency noises are still smaller than 1.0×10^{-20} A^2/Hz. Fig. 5(c) shows that the

dark currents of the AZO824-LED at zero bias and -3 V are at the order of 10^{-13} A (@0.12 mm^2). Under a purple LED (395 nm) illumination, photocurrents of the AZO824-LED within the voltage range less than 2 V increase with the optical powers of the purple LED by 6 orders of magnitude. The measured maximum photocurrent is around 1 μA.

Previously, a benchmark made on GaN-based visible light detectors was 1.28 A/W at 380 nm under a reverse bias 0.1 V, the corresponding product of quantum efficiency and gain was 572% [32]. At 400 nm, its responsivity decreased rapidly to below 0.1 A/W. Although the report didn't mention the FWHM value, it should be larger than 100 nm, deducing from Fig. 3 of [33]. Hence, this work places another landmark toward realizing true potentials of GaN-based visible light detectors for dense WDM VLC applications [32].

Worthy of mention is that the responsivity of AZO LEDs is sensitive to the chip structure. Except for the AZO824-LED, AZO-LEDs with other mesa sizes, such as 1000 μm $\times$ 1000 μm, 250 μm $\times$ 750 μm, 200 μm $\times$ 1000 μm, 200 μm $\times$ 200 μm and 150 μm $\times$ 150 μm, are fabricated and measured for comparison. All of them show lower optical responsivities than the AZO824-LED. Among them, the AZO-LEDs with mesa sizes of 250 μm $\times$ 750 μm and 200 μm $\times$ 1000 μm present a relatively higher responsivity, around 160 mA/W at 380 $\sim$ 400 nm. The underline mechanism is still not clear and may be related with resonant-cavity assisted multiplication processes, which deserves deep investigation to further increase the responsivity and narrow down the FWHM. Since previous studies have revealed that modulation bandwidth of a GaN PD is RC-limited, balances between response time and optical responsivity must be considered on chip structure optimization.

6. Proposition for Duplex VLCs

Different from previous work, as a generic structure, we propose to fabricate two AZO824-LEDs on a single chip, one as the light emitter (E-LED) and another as the light receiver (PD-LED). A Si-based PIN photodiode and a purple LED with a peak wavelength around 395 nm will be hybrid integrated together as an up-link device. The down-link VLC is conducted between the E-LED and the commercial Si-based PIN photodiode. The up-link VLC is conducted between the purple LED and the PD-LED. Since the peak wavelengths of the down-link and up-link lights have a difference around 50 nm and the light response of PD-LED exhibits a narrow band-pass (FWHM $=$ 60 nm), the optical cross-talk between simultaneously down-link and up-link communications can be largely inhibited naturally, i.e., the PD-LED bypassing the optical spectrum of the E-LED mostly. Fig. 6(a) summarizes the optical spectra of the E-LED and purple LED, the spectral responses of the PD-LED and the commercial Si-based PIN detector (New port 818-BB-21 A). The optical spectra of the E-LED and purple LED are normalized, while the spectral response curves represent the measured actual values. The responsivities of the Si PIN detector at 450 nm and 395 nm are around 150 mA/W and 100 mA/W, while the responsivities of the PD-LED at 450 nm and 395 nm are around several mA/W and 450 mA/W. Obviously, the commercial Si PIN detector is not the ideal choice. A narrow-band-pass PD with a higher peak responsivity at 450 nm (e.g., 0.3 $\sim$ 0.7 A/W) is needed. A block diagram is drawn in Fig. 6(b) to show the idea of duplex VLCs. In order to experimentally demonstrate duplex VLC performances, an amplifying circuit needs to be designed for PD-LED, which will be conducted in our future work through collaborations. Further work on high speed purple LED's design is going on. Additional collimating optics between the light emitter and receiver shall be introduced into to cope with different practical applications. In the following, we only preliminarily test the modulation performances of the fabricated AZO824-LED as a light emitter, i.e., the down-link channel in the proposition for bi-directional VLCs. The performances of PD-LED still need further improvement to narrow down the bandwidth for crosstalk reduction.

An intensity-modulation/direct-detection (IM/DD) transmitter-receiver VLC system is set up as reported in [30]. An orthogonal frequency division multiplexing (OFDM) scheme is developed to demonstrate the communication capability of the designed AZO824-LED as a light emitter. At

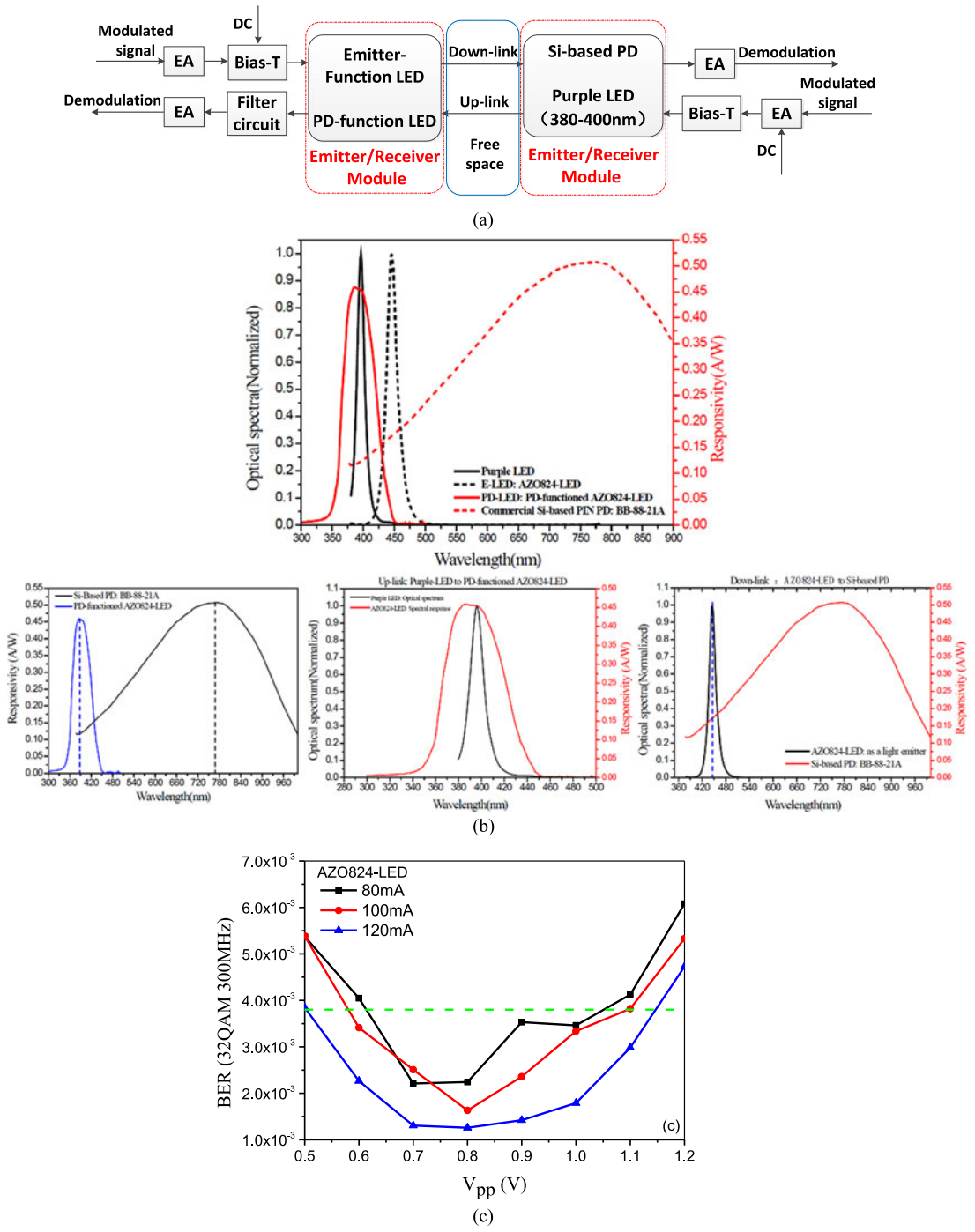

Fig. 6. (a) A block diagram showing the idea of duplex VLCs; (b) A comprehensive diagram is given first summarizing the optical spectra of the E-LED and purple LED, the spectral responses of the PD-LED and the commercial Si-based PIN detector (New port 818-BB-21 A); then, the spectral responsivity of Si-based PD(818-BB-21 A) and PD-functioned AZO824-LED are compared in a single figure(left); in the up-link channel, the normalized optical spectrum of purple LED emitter and the spectral responsivity of PD-functioned AZO824-LED receiver are plotted in a single figure(middle); in the down-link channel, the normalized optical spectrum of AZO824-LED emitter and the spectral responsivity of Si-based PD is plotted in a single figure(right). (c) Preliminary results on the down-link channel: the measured BER versus the V_{pp} values at different bias currents for AZO824-LED.

the transmitter side, the incoming binary sequences are modulated using quadrature amplitude modulation (QAM) format, and then sent into the OFDM encoder. The inverse fast Fourier transform (IFFT) is employed to generate QAM-OFDM signal. In this experiment, the QAM-OFDM signal consists of 128 subcarriers, and the up-sample factor is 3. So the utilized IFFT size is $128 * 3 = 384$. The cyclic prefix (CP) at the length of 1/16 symbol is added. The QAM-OFDM signal is generated by an AWG (Tektronix AWG710) at the sampling rate of 1.8 GS/s, and the modulation bandwidth is 300 MHz (from 18.75 MHz to 318.75 MHz). No pre-equalization operation is done on the signals. At the receiver side, a high speed silicon PIN detector (New port 818-BB-21 A, gain $= 1$) is used. And the detected signal is recorded by the oscilloscope (OSC, Agilent 54855 A: 6 GHz bandwidth) at 2 GS/s sampling rate. Then, the signal is down-sampled, CP moved and FFT. 10% training symbol is used for zero-forcing channel equalization. In order to reduce the multipath attenuation effects and test the real performances of AZO824-LED, the distance between the transmitter and the receiver is fixed at 5 cm. To simplify the system's optics for practical applications, the system doesn't adopt any microscope objective to collimate the light beams from the emitter.

The real free space communication capabilities of the fabricated AZO824-LEDs are demonstrated experimentally. 300 MHz 32 QAM OFDM signals are applied to a single AZO824-LED. The peak-to-peak voltages (V_{pp}) of modulating signals are set at $0.5 \sim 1.2$ V to utilize the full dynamic range of the AZO824-LED. The measured bit-error-rates (BER) versus the bias currents are drawn in Fig. 6(c). As the bias current increases from 80 mA to 120 mA, the BERs at all V_{pp} values decrease. A 1.5 Gbit/s speed is successfully achieved in a wide operation range under a pre-forward-error-correction (pre-FEC) threshold of 3.8×10^{-3}. The self-heating effect within the chip is not obvious at the current of $80 \sim 120$ mA, as can be seen from Fig. 4(b). The present work doesn't intend to explore the true free-space data transmission potential of the fabricated AZO824-LED, but to preliminarily prove that the generic bi-function LED doesn't sacrifice its performances as a light transmitter.

7. Conclusions and Remarks

In the present work, GaN-based generic bi-function LED is designed for potential duplex VLC applications, which has a 300 nm *n^+-ZnO* epitaxial layer grown on a standard GaN LED epi-stack. As a photodetector, the fabricated AZO824-LED exhibits a peak responsivity of 450 mA/W at $380 \sim 400$ nm under zero bias. The corresponding product of quantum efficiency and gain is estimated as 140%. The purple light ($380 \sim 400$ nm) to blue light (>460 nm) rejection ratio can reach two orders of magnitude. To the best of authors' knowledge, the obtained responsivity at $380 \sim 400$ nm is highest for the state of art. The FWHM of the response spectrum is relatively narrow, around 60 nm. This result places a landmark toward realizing true potentials of GaN-based visible light detectors for dense WDM VLC applications. As a light emitter, the AZO824-LED exhibits an optical power reaching 100 mW with a peak wavelength around 447 nm. Experimentally, based on a fix-rate OFDM modulation scheme without pre-equalization processing, a modulation bandwidth of 300 MHz and a free space data speed 1.5 Gb/s are demonstrated by a single down-link between an AZO824-LED and a Si-based PIN PD at a distance of 5 cm. The present work doesn't intend to explore the true free-space data transmission potential of the fabricated AZO824-LED, but to preliminarily prove that the generic bi-function LED doesn't sacrifice its performances as a light transmitter.

Although the crosstalk between the optical responsivity spectra of PD-LED and the light emitting spectra of E-LED is largely inhibited, it is still far from perfect. Performances of the GaN-based generic bi-function LED epi-stack need further improvement for realizing duplex VLCs.

References

[1] H. Elgala, R. Mesleh, and H. Haas, "Indoor optical wireless communication: Potential and state-of-art," *IEEE Commun. Mag.*, vol. 49, no. 9, pp. 56–62, Sep. 2011.

[2] D. O'Brien, G. Parry, and P. Stavrinou, "Optical hotspots speed up wireless communication," *Nature Photon.*, vol. 1, pp. 245–247, May 2007.

[3] D. O'Brien, L. Zeng, H. Le-Minh, G. Faulkner, J. W. Walewski, and S. Randel, "Visible light communications: Challenges and possibilities," in *Proc. IEEE 19th Int. Symp. Pers., Indoor, Mobile Radio Commun.*, Sep. 2008, pp. 1–5.
[4] K. Toshihiko and M. Nakagawa, "Fundamental analysis for visible-light communication system using LED lights," *IEEE Trans. Consum. Electron.*, vol. 50, no. 1, pp. 100–107, Feb. 2004.
[5] G. Cossu, A. M. Khalid, P. Choudhury, R. Corsini, and E. Ciaramella, "3.4 Gbit/s visible optical wireless transmission based on RGB LED," *Opt. Exp.*, vol. 21, no. 1, pp. 1203–1208, 2013.
[6] J. Y. Sung, C. W. Chow, and C. H. Yeh, "Dimming-discrete-multi-tone(DMT) for simultaneous color control and high speed visible light communication," *Opt. Exp.*, vol. 22, no. 7, pp. 7538–7543, 2014.
[7] S. Muthu, F. J. P. Schuurmans, and M. D. Pashley, "Red, green, and blue LEDs for white light illumination," *IEEE J. Sel. Topics Quantum Electron.*, vol. 8, no. 2, pp. 333–338, Mar./Apr. 2002.
[8] F. C. Wang, C. W. Tang, and B. J. Huang, "Multivariable robust control for a red-green-blue LED lighting system," *IEEE Trans. Power Electron.*, vol. 25, no. 2, pp. 417–428, Feb. 2010.
[9] N. Chi, Y. Wang, Y. Wang, X. Huang, and X. Lu, "Ultra-high-speed single red-green-blue light-emitting diode-based visible light communication system utilizing advanced modulation formats," *Chin. Opt. Lett.*, vol. 12, no. 1, 2014, Art. no. 010605.
[10] Y. Wang, X. Huang, J. Zhang, Y. Wang, and N. Chi, "Enhanced performance of visible light communication employing 512QAM N-SC-FDE and DD-LMS," *Opt. Exp.*, vol. 22, no. 13, pp. 15328–15334, 2014.
[11] Y. Wang, X. Huang, L. Tao, J. Shi, and N. Chi, "4.5-Gb/s RGB-LED based WDM visible light communication system employing CAP modulation and RLS based adaptive equalization," *Opt. Exp.*, vol. 23, no. 10, pp. 13626–13633, 2015.
[12] Y. G. Wang, T. Li, X. X. Huang, J. Y. Shi, and N. Chi, "8-Gb/s RGBY LED-based WDM VLC system employing high-order CAP modulation and hybrid post equalizer," *IEEE Photon. J.*, vol. 7, no. 6, Dec. 2015, Art. no. 7904507.
[13] C. H. Yeh *et al.*, "Utilization of multi-band OFDM modulation to increase traffic rate of phosphor-LED wireless VLC," *Opt. Exp.*, vol. 23, pp. 1133–1138, 2015.
[14] C. W. Chow, C. H. Yeh, Y. F. Liu, and P. Y. Huang, "Background optical noises circumvention in LED optical wireless systems using OFDM," *IEEE Photon. J.*, vol. 5, no. 2, Apr. 2013, Art. no. 7900709.
[15] J. R. D Retamal *et al.*, "4-Gbit/s visible light communication link based on 16-QAM OFDM transmission over remote phosphor-film converted white light by using blue laser diode," *Opt. Exp.*, vol. 23, no. 26, pp. 33656–33666, 2015.
[16] Y. C. Chi *et al.*, "Phosphorous diffuser diverged blue laser diode for indoor lighting and communication," *Sci. Rep.*, vol. 5, 2015, Art. no. 18690.
[17] X. X. Huang, Z. X. Wang, J. Y. Shi, Y. G. Wang, and N. Chi, "1.6 Gbit/s phosphorescent white LED based VLC transmission using a cascaded pre-equalization circuit and a differential outputs PIN receiver," *Opt. Exp.*, vol. 23, pp. 22034–22042, 2015.
[18] S. Wang *et al.*, "A high-performance blue filter for a white-LED-based visible light communication system," *IEEE Wireless Commun.*, vol. 22, no. 2, pp. 61–67, Apr. 2015.
[19] X. X. Huang *et al.*, "2.0-Gb/s visible light link based on adaptive bit allocation OFDM of a single phosphorescent white LED," *IEEE Photon. J.*, vol. 7, no. 5, Oct. 2015, Art. no. 7904008.
[20] A. M. Cailean and M. Dimian, "Current challenges for visible light communications usage in vehicle applications: A survey," *IEEE Commun. Surveys Tut.*, no. 99, May. 2017. doi:10.1109/COMST.2017.2706940.
[21] Y. J. Wang *et al.*, "Simultaneous light emission and detection of InGaN/GaN multiple quantum well diodes for in-plane visible light communication," *Opt. Commun.*, vol. 387, no. 15, pp. 440–445, 2017.
[22] G. Cossu, A. Wajahat, R. Corsini, and E. Ciaramella, "5.6 Gb/s downlink and 1.5 Gb/s uplink optical wireless transmission at indoor distance(1.5 m)," in *Proc. 40th Eur. Conf Opt. Commun.*, Sep. 21–25, 2014, pp. 1–3.
[23] Y. Q. Wang, Y. G. Wang, N. Chi, J. J. Yu, and H. L. Shang, "Demonstration of 575Mb/s downlink and 225 Mb/s uplink bi-directional SCM-WDM visible light communication using RGB LED and phosphor-based LED," *Opt. Exp.*, vol. 21, no. 1, pp. 1203–1208, 2013.
[24] Z. Y. Jiang *et al.*, "Monolithic integration of nitride light emitting diodes and photodetectors for bi-directional optical communication," *Opt. Lett.*, vol. 39, no. 19, pp. 5657–5660, 2014.
[25] E. Miyazaki, S. Itami, and T. Araki, "Using a light-emitting diode as a high-speed, wavelength selective photodetector," *Rev. Sci. Instrum.*, vol. 69, no. 11, pp. 3751–3754, 1998.
[26] F. Capasso, K. Mohammed, A. Y. Cho, R. Hull, and A. L. Hutchinson, "New quantum photoconductivity and large photocurrent gain by effective-mass filtering in a forward-biased superlattice p-n junction," *Phys. Rev. Lett.*, vol. 55, pp. 1152–1155, 1985.
[27] C. Rivera, J. L. Pau, and E. Munoz, "Photocurrent gain mechanism in schottky barrier photodiodes with negative average electric field," *Appl. Phys. Lett.*, vol. 89, 2006, Art. no. 263505.
[28] J. Pereiro *et al.*, "Optimization of InGaN-GaN MQW photodetector structures for high-responsivity performance," *IEEE J. Quantum Electron.*, vol. 45, no. 6, pp. 617–622, Jun. 2009.
[29] G. Stepniak, M. Kowalczyk, L. Maksymiuk, and J. Siuzdak, "Transmission beyond 100Mbit/s using LED both as a transmitter and receiver," *IEEE Photon. Technol. Lett.*, vol. 27, no. 19, pp. 2067–2070, Oct. 2015.
[30] Z. K. Sun *et al.*, "A power-type single GaN-based blue LED with improved linearity for 3 Gb/s free-space VLC without pre-equalization," *IEEE Photon. J.*, vol. 8, no. 3, Jun. 2016, Art. no. 7904308.
[31] F. Akyol, S. Krishnamoorthy, and S. Rajan,"Tunneling-based carrier regeneration in cascaded GaN light emitting diodes to overcome efficiency droop," *Appl. Phys. Lett.*, vol. 103, no. 8, 2013, Art. no. 081107.
[32] D. D. Teng, M. Y. Wu, L. L. Liu, and G. Wang, "Size- and current-density-controlled tunable wavelength in GaN-based LEDs for potential dense wavelength-division multiplexing application," *IEEE Wireless Commun.*, vol. 22, no. 2, pp. 74–79, Apr. 2015.
[33] Y. Z. Chiou *et al.*, "High detectivity InGaN-GaN multiquantum well p-n junction photodiodes," *IEEE J. Quantum Electron.*, vol. 39, no. 5, pp. 681–685, May 2003.